Muscle Spindle Model-Based Non-Invasive Electrical Stimulation for Motion Perception Feedback in Prosthetic Hands*

Chenyu Tong, Bicen Yan, Dongxu Liu, and Qichuan Ding, *Member, IEEE*

***Abstract*—Prosthetic hands offer significant benefits for patients with hand amputations by partially replicating the functionality of real hands. However, most current prosthetics lack sensory feedback on movement, leading to a gap in proprioception for users. To bridge this gap and approximate the natural experience of hand use, prosthetic hands must offer detailed motion feedback. This paper introduces a non-invasive electrical stimulation approach aimed at providing motion perception feedback through modeling muscle spindles. By employing transcutaneous electrical nerve stimulation (TENS), the method generates artificial sensory signals, potentially restoring a degree of proprioception for users. We developed an experimental framework involving an electronic prosthetic hand, an electrical stimulator, and surface electrodes to assess our approach. Preliminary experiments with six participants, including one with a hand amputation, indicate that users can discern the movement angle of a prosthetic hand with a fair degree of accuracy. These findings suggest the viability of our method in creating prostheses with enhanced proprioceptive feedback.**

I. Introduction

Losing hands can greatly affect the quality of life of patients with palmar amputations. Those amputees often need to rely on prosthetic hands to regain some level of hand functionality. The increasing demands for advanced prostheses have also prompted the evolution of prosthetic technology from basic switch controls to more sophisticated autonomous systems. As a representative of autonomously controlled prostheses, myoelectric prosthesis has attracted widespread attention [1]. Myoelectric prostheses allow amputees to regain voluntary movement control of artificial limbs by utilizing the surface electromyographic signal acquired from residual muscles [2]. However, most current prostheses can only achieve a downstream control from brain to artificial limbs, lacking of the upward perception of the movement status of artificial limbs, i.e., the feedback from limbs to brain. Overreliance on visual cues to obtain the movements of artificial limbs results in a lack of proprioception in operating prostheses [3].

Proprioception allows humans to move limbs in a smooth and coordinated manner, learn new motor skills, and move limbs without visual surveillance [4]. Therefore, reliable, real-time, and natural feedback to users is a key to enhancing the proprioception of prostheses [5]. In recent years, the rapid developments of neural interfaces for the peripheral nervous system present a promising solution. Prosthesis can bi-directionally communicate with residual limb nerves of amputees through neural interfaces, thereby restoring the natural flow of proprioceptive information [6]. Neural interfaces used for prostheses mainly include two types, i.e., invasive and non-invasive (wearable). Current studies have shown that both interaction technologies can provide certain sensory feedback for users [7-8]. Edoardo D Anna et al. have demonstrated the feasibility of invasive interfaces by implanting transverse intrafascicular multi-channel electrodes (TIME) in the ulnar and median nerves of transradial amputees, providing them with feedback on hand movements during grasping tasks [7]. However, the necessity for surgical implantation of electrodes makes invasive approaches potentially traumatic for users.

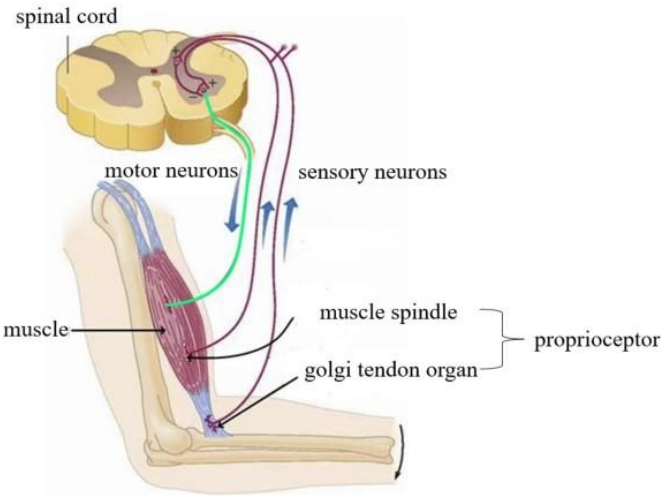

Figure 1. principles of proprioception

In contrast, non-invasive neural interfaces, when paired with prostheses, offer a safer and more practical alternative for delivering sensory feedback, with significant potential for commercialization. Semyoung Oh et al. successfully transmitted elbow joint flexion angle information to subjects through a non-invasive neural interface (e-skin), underscoring the viability of non-invasive methods [8]. Their study established a correlation between the elbow joint angles and the stimulation current frequency, enabling subjects to differentiate feedback corresponding to various joint angles. However, the approach did not emulate the real neural discharge patterns associated with proprioception, instead relying on empirical rules to modulate the stimulation current frequency. This method does not have a strong physiological basis, highlighting a pressing challenge in the field: aligning

* Research supported in part by the National Natural Science Foundation of China under Grant 62373086 and Grant 62373087, and Guangdong Basic and Applied Basic Research.

C. Tong, B. Yan and D. Liu are with the Faculty of Robot Science and Engineering, Northeastern University, Shenyang 110169, China.

Q. Ding is with the Faculty of Robot Science and Engineering, Northeastern University, Shenyang 110169, China, and with Foshan Graduate School of Innovation, Northeastern University, Foshan 528311, China (e-mail: dingqichuan@mail.neu.edu.cn)

Manuscript 516 submitted to 2024 IEEE/RSJ International Conference on Intelligent Robots and Systems (IROS). Received February 28, 2024.

simulated sensory feedback more closely with the natural sensory experiences remains an unresolved issue.

In this paper, we explore the foundational principles of proprioception, revealing the pivotal role of proprioceptors in sensory feedback. These receptors, activated by movements of joints, muscles and tendons, transform motion data into neural signals. The signals of receptors are then relayed to the brain via the nervous system, facilitating proprioceptive perception [9] (Fig.1). Consequently, this paper proposes a novel approach: building a proprioceptor model to simulate the neural firing patterns of the receptor. By combining the model with non-invasive neural interfaces, we aim to offer prosthetic users more natural and realistic proprioceptive information.

As the most important proprioceptor of human body, muscle spindle can sensor changes in muscle length and the velocity of stretching, providing critical feedback for precise movement control during physical activities [10]. Consequently, we have selected the muscle spindle as the primary physiological receptor, developing a transfer model that replicates its response to nerve electrical signals. This model, integrated with non-invasive neural interfaces, forms the basis of our proprioceptive prosthetic hand framework. Building on this foundation, we have constructed a proprioceptive prosthetic hand capable of converting joint angle data, into electrical stimuli. This innovative approach aims to deliver a proprioceptive experience that closely resembles natural sensation, enhancing the control and interaction of users with the prosthetic.

Preliminary experiments were conducted on six participants, including one with a hand amputation, to verify the efficacy of our approach. The experimental results, especially regarding the sensory perception of the participants on the motion angles of the prosthetic hand, demonstrate the viability of our approach in facilitating motion perception feedback.

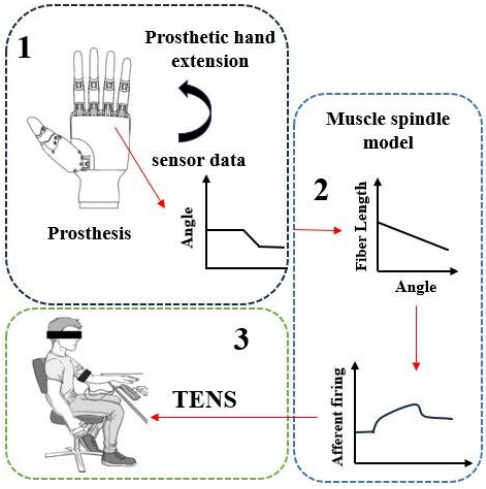

Figure 2. The framework of the proposed proprioceptive prosthetic hand

II. METHOD

The framework of our proprioceptive prosthetic hand consists of three primary components: (1) Electronic prosthetic hand, equipped with sensors that can capture the angles of the metacarpophalangeal joints; (2) Muscle spindle model, converting sensor data into neural firing patterns that mimic those produced by natural proprioceptive receptors in human body; (3) Electric stimulator, utilizing transcutaneous electrical stimulation (TENS) to transmit the sensory information generated by the muscle spindle model directly to the human nervous system. Fig.2 illustrates the framework of the proprioceptive prosthetic hand. In this section, we will primarily discuss muscle spindles and muscle spindle models, while the hardware components of the system will be introduced in the experiment.

A. Muscle Spindle

Muscle spindles are distributed throughout mammalian skeletal muscles and serve as the main source of proprioceptive feedback for spinal sensorimotor regulation [11]. Muscle spindles are composed of three types of intrafusal fibers: dynamic nuclear bag fibers (bag1), static nuclear bag fibers (bag2) and nuclear chain fibers (chain). Dynamic nuclear bag fibers are particularly sensitive to variations in muscle length, whereas static nuclear bag fibers and nuclear chain fibers respond more significantly to the absolute length of the muscle [12]. The primary sensory nerves (Ia), responsible for conveying rapid feedback, are situated in the central regions of the three types of intrafusal fibers. In contrast, the secondary sensory nerves (II), which conduct impulses more slowly, are located at the ends of the static bag fibers and chain fibers, providing sustained feedback on muscle stretch, as illustrated in Fig.3.

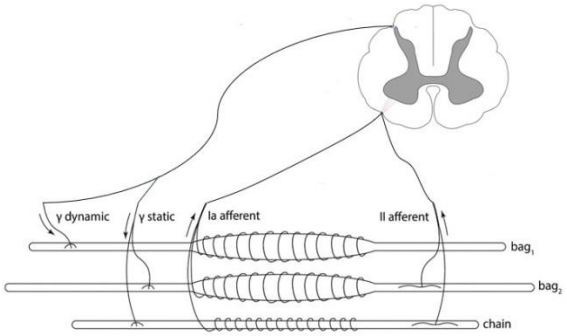

Figure 3. A biological muscle spindle consists of 3 types of intrafusal fibers that receive several fusimotor inputs (gamma static and dynamic) while giving rise to primary (Ia) and secondary (II) afferent.

Muscle spindles play a crucial role during muscle stretch and contraction, adjusting the rate of action potentials fired by the intrafusal fibers. Subsequently, the nerve electrical signals generated in the intrafusal fibers are transmitted to the central nervous system through the primary (Ia) and the secondary (II) afferent nerve, enabling human to perceive the position and speed of limb movement [13].

Based on the experimental results in published in the [14], the frequency of electrical signals in primary afferent nerves undergoes more pronounced changes during muscle fiber stretching and contraction. Conversely, secondary afferent nerves lack connectivity with dynamic nuclear bag fibers, and do not convey information regarding the rate of muscle length change to the central nervous system. Thus, we only consider the firing rate of primary afferent nerves as the sole output of the muscle spindle system, disregarding the influence of secondary afferent activity.

Manuscript 516 submitted to 2024 IEEE/RSJ International Conference on Intelligent Robots and Systems (IROS). Received February 28, 2024.

B. Muscle Spindle Model

Researchers have sought to employ mathematical models to characterize muscle spindle activities. Among these models, the Rudjord model effectively describes the primary afferent activity of muscle spindles [15].

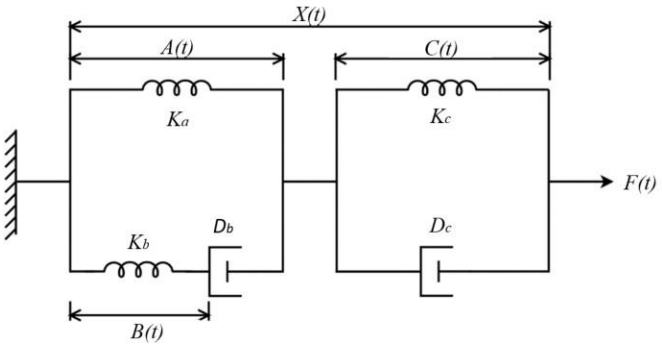

Figure 4. Second order mechanical model of primary endings of mammalian muscle spindles

The network is shown in Fig. 4, in which the pure elastic element K_a represents the mechanical effect of the fibers within the nuclear chain shuttle, and the Maxwell elements K_b and D_b reflect the mechanical properties of the central region of the bag fiber. The Voigt elements K_c and D_c take into account the viscoelastic behavior of the fiber polar region within the muscle spindle. When changes in muscle fiber length $X(t)$ act on the entire system, corresponding changes in length ($A(t)$ and $B(t)$) of elastic elements K_a and K_b are thought to activate afferent activity in chain and bag fibers. $F(t)$ is the equivalent muscle force. The output components of the above two incoming activities are superimposed in a certain proportion and become the output of the system (the proportion is set to 1 in this study). Finally, the transfer function of the overall muscle spindle system is obtained, the formula is derived as follows:

$$K_c C(s) + sD_c C(s) = K_a A(s) + K_b B(s) \quad (1)$$

$$K_b B(s) = sD_b (A(s) - B(s)) \quad (2)$$

Equations (1) and (2) represent the equations of motion applied to the entire system and to the nuclear bag fiber branches, respectively. Besides, the total length of the system is given by,

$$X(s) = A(s) + C(s) \quad (3)$$

The transfer function of the entire system can be expressed by the superposition of the transfer functions of the afferent activity of the nuclear bag fiber branches and the afferent activity of the nuclear chain fibers:

$$H(s) = H_a(s) + H_b(s) \quad (4)$$

$$H_a(s) = \frac{A(s)}{X(s)},\ H_b(s) = \frac{B(s)}{X(s)} \quad (5)$$

The transfer function of the muscle spindle model can be obtained:

$$H(s) = \frac{1 + (\frac{D_b}{D_c} + \frac{D_b + D_c}{K_a + K_c})s + \frac{D_b D_c}{K_b (K_a + K_c)} s^2}{1 + (\frac{D_c}{K_c} + \frac{2D_b}{K_b})s + \frac{2D_b D_c}{K_b K_c} s^2} \quad (6)$$

For efficient implementation, we employ a bilinear transformation with a sampling frequency of 100 Hz to convert the transfer function of the model into the *z*-domain. Subsequently, we substitute a set of parameter values published by Rudjord in the paper [15] to derive the transfer function of the muscle spindle model in the *z*-domain:

$$H(z) = \frac{7.8 + 0.126176 z^{-1} - 7.6445\, z^{-2}}{1 + 0.112676 z^{-1} - 0.831 z^{-2}} \quad (7)$$

Equation (7) represents a muscle spindle model with muscle fiber length as the only independent variable and discharge frequency as the dependent variable. However, the prosthetic hand outputs the movement angles with its internally integrated angle sensor. To effectively integrate the prosthetic hand with the muscle spindle model, it is necessary to convert the joint angle information into muscle fiber length information.

When the palm naturally flexes, the metacarpophalangeal and interphalangeal joints move correspondingly, thereby stretching or contracting the corresponding flexor muscles of the forearm (like the flexor digitorum profundus). However, we have observed that finger movements involve various muscles, and the specific muscles engaged differ for each finger [16]. This process is too complicated to facilitate the implementation of the system. Here, we aim to establish a simple relationship between joint angle and muscle length.

Williams et al. compiled data on the elbow joint angle and brachialis muscle fiber length in [17]. In order to simplify calculations, this paper conducted linear regression analysis on the available data, resulting in a model that describes the relationship between muscle fiber length and joint angle (Fig. 5).

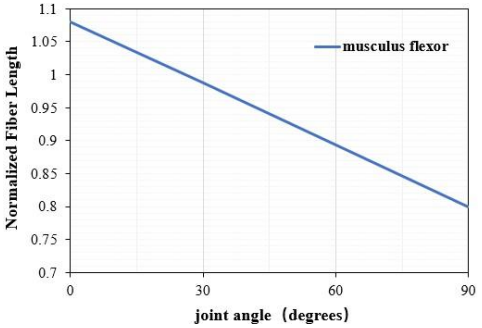

Figure 5. The linear regression model describing the relationship between joint angles and muscle length.

C. Muscle Spindle Model Output Curve

The implementation process of the entire system (Fig.2) and the muscle spindle model has been described in the preceding sections. This section will now present the output results of the muscle spindle model.

Manuscript 516 submitted to 2024 IEEE/RSJ International Conference on Intelligent Robots and Systems (IROS). Received February 28, 2024.

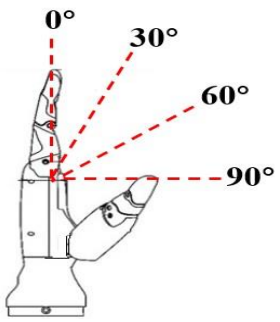

Figure 6. The illustration of the angle distribution of the prosthetic hand fingers.

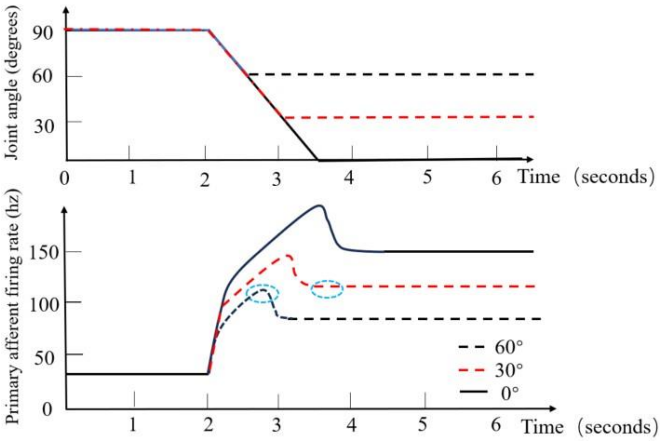

Figure 7. The output curves of the muscle spindle model when the hand moves from the position of 90°to the positions of 60°, 30° and 0°.

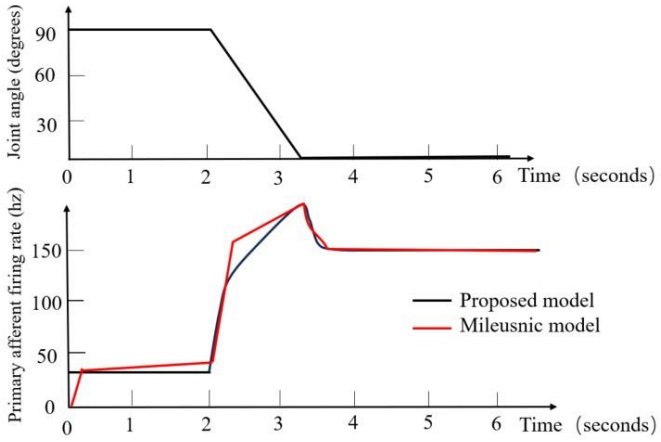

Figure 8. The muscle spindle model proposed in this paper is compared with the model proposed by Mileusnic.

We test the ability of the muscle spindle model to capture the movement angle of prosthetic hand fingers. First, the prosthetic hand was driven to move from the position of 90° to the positions of 60°, 30°, and 0° at a consistent speed (60°/s), and draw the output curve corresponding to the muscle spindle model. Fig. 6 illustrates the joint angles of the prosthetic hand. Fig. 7 illustrates the muscle spindle model's output at different angles of the metacarpophalangeal joint. To assess the accuracy of the muscle spindle model, a comparison was made with the output results of the Mileusnic model (see Fig.8). The Mileusnic model has been parameterized and validated using cat muscle spindle recordings detailed in published literature [14]. Based on our findings, we assert that the muscle spindle model proposed in this paper offers a comprehensive depiction of the afferent activity within the muscle spindle system.

III. Experiment

A. Human Subjects Recruitment

Five healthy subjects, including 3 males and 2 females, with a mean age of 23.7 ± 0.5, and a 50-year-old male hand amputation patient (amputated 8 years ago), were recruited to participate in our experiments. Prior to participation, all participants were fully informed about the experimental procedures and provided their informed consent by signing a consent form. The experiments were conducted in compliance with relevant guidelines and regulations, following approved protocols from Northeastern University. Throughout the electrical stimulation procedures, the subjects were seated comfortably in a chair in front of a table, with their arms resting naturally on the table in a palms-up position. Two electrodes are attached to the surface of two muscles of the forearm, i.e., the brachioradialis and flexor carpi ulnaris muscles.

B. System Hardware

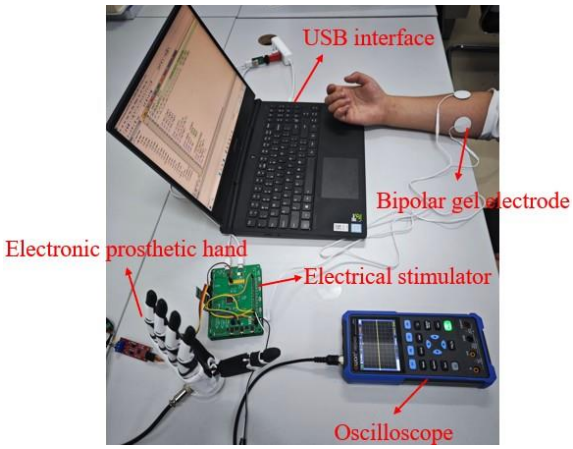

Figure 9. System hardware components for sensory information feedback. Includes electronic prosthetic hand, bipolar gel electrodes, electrical stimulator, oscilloscope and computer for programming.

The system hardware is depicted in Fig.9. Here, the movement angle information of the electric prosthetic hand is conveyed to the human nervous system through TENS. The electrical stimulator consists of two key components: an electrical stimulation chip responsible for generating electrical stimulation pulses, and a main control chip that regulates the output of the electrical stimulation chip based on real-time information. The implementation program of muscle spindle model was integrated in the main control chip. As the electronic prosthetic hand undergoes movement, its internal angle sensor promptly transmits real-time data to the main control chip, which is then converted into a firing rate. Subsequently, the main control chip regulates the electrical stimulation chip to emit electrical signals at this rate, thereby stimulating the forearm flexors of subjects through bipolar gel surface electrodes.

C. Determine Electrical Stimulation Parameters

Kajimoto et al. demonstrated that biphasic stimulation can aid in mitigating cellular responses and preventing ion uptake

from electrodes and conductive gels [18]. In addition, the experiments in [19] revealed that a pulse width of approximately 100 μs offers an optimal balance between power consumption and receptor stimulation [19]. Consequently, this study employed bipolar electrical stimulation pulses with a pulse width of 100 μs .

In transcutaneous electrical nerve stimulation, the stimulation amplitude is an important parameter. To ensure the safety of each subject, it is necessary to establish the stimulation amplitude for each subject prior to the formal experiment. Refer to the research conducted by Geng et al. [20], we propose a method to determine the stimulus amplitude during the experimental phase. Specifically, we measured the perception threshold and the discomfort threshold of each subject.

First, we increased the amplitude of the stimulation current from 0 by three different increments (0.1 mA , 0.2 mA , 0.3 mA) to obtain three preliminary estimations of the perception threshold (the value at which the subject can initially feel electric stimulation). The average of the three values was then taken as the perception threshold of the subject. Second, we used the perception threshold as the initial amplitude to increase the stimulation amplitude until the subject felt pain, with the step length of the increment selected in the range between 0.2 mA and 0.4 mA . The experiment was repeated three times, and the average of the three results was the discomfort threshold of the subject. Third, the average of the perception threshold and the discomfort threshold was used as the stimulus amplitude suitable for the subject in the following experiment.

D. Sensory and Movement Adaptation Training

The sensory and movement adaptation training was conducted to fit the sensory of each subject in perceiving the movement angles of prosthetic hand fingers. During the adaptation training, the subjects visually observed the movement of the prosthetic hand. The operator controlled the metacarpophalangeal joints of the prosthetic hand to sequentially move to the positions of 0°, 30°, 60°, and 90°. Simultaneously, the electrical stimulator emitted electrical signals at corresponding frequencies, providing different sensory information to the subjects. Based on visual feedback, the subjects matched sensory information with joint angles. Each subject underwent 12 adaptation training sessions, with each joint angle trained three times. After the training, the subjects were allowed to rest for 3 minutes.

E. Sensory and Movement Matching Test

During the sensory and movement matching test, we asked the subject to wear a blindfold to block the visual feedback. The operator controls the prosthetic hand to flex to different angles according to a random order. Subjects did not know the movement order of the prosthetic hand, and each angle was presented 5 times. After the metacarpophalangeal joint reached to a specific angle, the subject replied the angle value to the operator only based on his/her sensory. The operator then controlled the metacarpophalangeal joint of the prosthetic hand to move to the next position, and the subject continued to complete the reply. The interval between each operation was 3 seconds. Six subjects participated in the experiment independently, ensuring that they did not communicate with each other. Fig.10 shows the sequence of the entire electrical stimulation experiment. Fig.11 shows the disabled subject being tested.

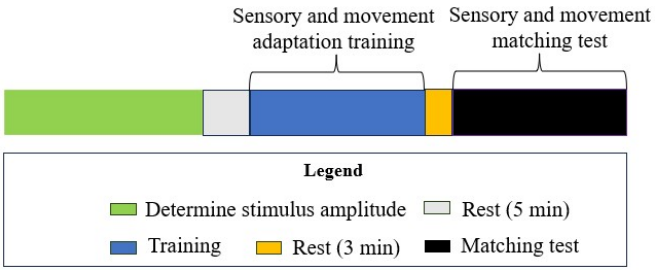

Figure 10. Schematic diagram of the overall electrical stimulation experiment sequence in this article

Figure 11. Matching test for a patient with amputation of hand

IV. Experimental Results

A. Selected Stimulation Amplitude for TENS

We measured the perception threshold and discomfort threshold for six subjects, resulting in the corresponding stimulation amplitudes for each subject. Detailed data can be found in Table 1.

TABLE I. ETERMINATION OF STIMULUS AMPLITUDES FOR FIVE SUBJECTS

Subject name	**Stimulation Amplitude for TENS**		
	Perception Threshold	***Discomfort Threshold***	***Stimulation Amplitude***
Subject 1	2.7mA	17.3mA	10.0mA
Subject 2	3.0mA	17.8mA	10.4mA
Subject 3	3.0mA	18.2mA	10.6mA
Subject 4	2.8mA	17.6mA	10.2mA
Subject 5	3.1mA	18.1mA	10.6mA
Subject 6*	3.6mA	19mA	11.3mA

a. Subject 6* is a hand amputation patient.

The data presented in Table 1 indicates that the sensory threshold for healthy participants generally ranged from 2.7 mA to 3.1 mA , with an average value of 2.92 mA , while the discomfort threshold ranged from 17.3 mA to 18.2 mA , with

an average value of 17.8 *mA* . In contrast, for the disabled participants, a measured sensory threshold was 3.6 *mA* and a discomfort threshold was 19 *mA* . Based on these findings, it can be inferred that the disabled participant received a higher stimulus amplitude during the experiment compared to his healthy counterparts. This observation seems to indicate that amputees may have higher perception thresholds for electrical stimulation due to prolonged closure of the sensory pathways of the nerves in the residual limb. Additionally, it is worth considering the potential influence of age, as the disabled participant was older than other healthy subjects. Subsequent studies should delve into the factors contributing to higher sensory thresholds and discomfort thresholds among disabled individuals.

B. Results of Matching Test

This study examined the potential of the proprioceptive prosthetic hand in providing motion perception feedback to the human body through the sensory and movement matching test. Fig.12 illustrates the responses of the six subjects to joint angles of 0°, 30°, 60°, and 90°, along with the perception accuracy average across all subjects for each angle. The average perception accuracy for subjects at 0°, 30°, 60°, and 90° was 100%, 90%, 86.7%, and 96.7%, respectively.

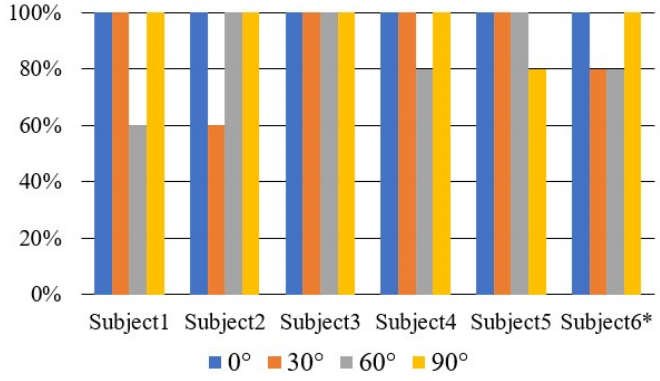

(a)

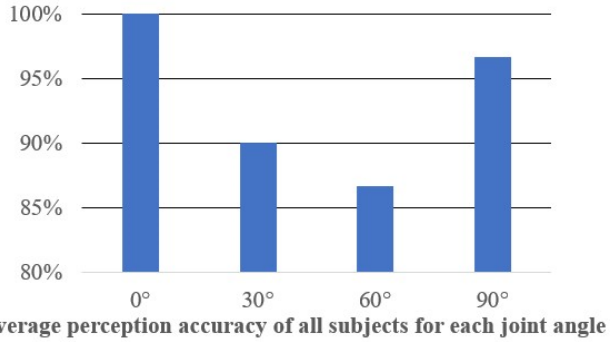

(b)

Figure 12. The perception results of six subjects for the movement of the prosthetic hand. (a) The perception accuracy of six subjects for joint angles of 30°, 60° and 90° respectively, and (b) the average perception accuracy of all subjects for 0°, 30°, 60° and 90°.

The sensory and movement matching test results revealed that all subjects were able to successfully discriminate sensory information at a joint angle of 0°. The relatively weak electrical stimulation sensation experienced by the subjects at the 0° joint angle made it easier for subjects to differentiate. Similarly, the perception of electrical stimulation is strongest at the joint angle of 90°, resulting in a relatively high accuracy of perception (96.7%) for this angle. Fig.13 presents the confused matrix of the perception matching across all subjects. From Figs.12 and 13, we can see that the subjects occasionally confuse sensory information at joint angles of 30° and 60°. The participants might find it challenging to discriminate when there are changes in electrical pulse frequency within the intermediate range.

Furthermore, note that in the muscle spindle model output curve presented in Fig. 7, the close response values can be observed between the frequency peak of the muscle spindle model during the dynamic response stage as the joint angle transitions from 90° to 60° and the static frequency values of the muscle spindle models at a joint angle of 30° (as plot by the two blue dash circles). This similarity may contribute to the confusion experienced by subjects when distinguishing sensory information at 30° and 60°. Therefore, the impact of these factors should be further explored in subsequent research.

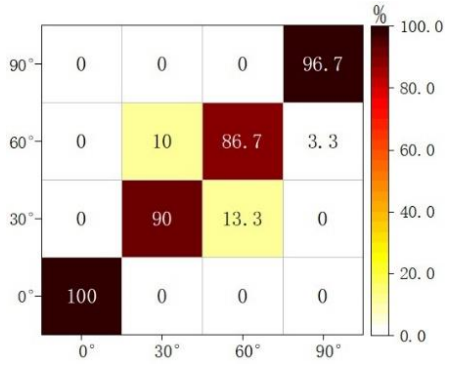

Figure 13. Confusion matrix of six subjects' perception accuracy for 4 joint angles.

C. System Stability and Subjects Post-feeling

After multiple flexions/extensions of the metacarpophalangeal joints, the sensors and surface electrodes all functioned normally. Moreover, after multiple movements of the electronic prosthetic hand, the perception threshold and discomfort threshold of the same subject hardly changed. Additionally, all subjects had no discomfort after completing all electrical stimulation experiments.

D. Limitations and Future Direction

This study had a limited number of participants, with only six subjects, including a single amputee. To investigate the stability of the proposed approach, future studies should consider increasing the number of participants. At the same time, we can invite more hand amputee patients to divide disabled subjects and normal subjects into two groups of equal numbers for comparative experiments. Furthermore, the current experimental design featured a relatively short time interval between matching training and matching testing, potentially overlooking the aftereffects of matching training. To address this, future investigations should incorporate longer time intervals to explore the lasting effects of electrical stimulation training.

V. Conclusion

This study introduces a novel approach to impart proprioceptive information to the human body. By developing a muscle spindle model and utilizing TENS to replicate the natural nerve discharge pattern of muscle spindles, the movement data of the electronic prosthetic hand is transformed into corresponding neuroelectric signals and transmitted to the human nervous system. This process aids the subjects in regaining a certain level of proprioception. Additionally, the conducted experiments have validated the efficacy of this method in providing motion perception feedback to the human body.

References

[1] M. Markovic, M. Varel, M. A. Schweisfurth, A. F. Schilling, and S. Dosen, "Closed-Loop Multi-Amplitude Control for Robust and Dexterous Performance of Myoelectric Prosthesis," *IEEE Trans. Neural Syst. Rehabil. Eng.*, vol. 28, no. 2, pp. 498–507, Feb. 2020.

[2] A. Furui *et al.*, "A myoelectric prosthetic hand with muscle synergy–based motion determination and impedance model–based biomimetic control," *Sci. Robot.*, vol. 4, no. 31, p. eaaw6339, Jun. 2019.

[3] P. D. Ganzer *et al.*, "Restoring the Sense of Touch Using a Sensorimotor Demultiplexing Neural Interface," *Cell*, vol. 181, no. 4, pp. 763-773.e12, May 2020.

[4] R. Rangwani and H. Park, "A new approach of inducing proprioceptive illusion by transcutaneous electrical stimulation," *J. NeuroEngineering Rehabil.*, vol. 18, no. 1, p. 73, May 2021.

[5] I. Williams and T. G. Constandinou, "Computationally efficient modeling of proprioceptive signals in the upper limb for prostheses: a simulation study," *Front. Neurosci.*, vol. 8, Jun. 2014.

[6] M. Zhang, Z. Tang, X. Liu, and J. Van Der Spiegel, "Electronic neural interfaces," *Nat. Electron.*, vol. 3, no. 4, pp. 191–200, Apr. 2020.

[7] E. D'Anna *et al.*, "A closed-loop hand prosthesis with simultaneous intraneural tactile and position feedback," *Sci. Robot.*, 2019.

[8] S. Oh, J. L. Patton, and H. Park, "Electro-prosthetic E-skin Successfully Delivers Elbow Joint Angle Information by Electro-prosthetic Proprioception (EPP)," in *2022 44th Annual International Conference of the IEEE Engineering in Medicine & Biology Society (EMBC)*, Glasgow, Scotland, United Kingdom, Jul. 2022, pp. 1485–1488.

[9] B. P. Delhaye, K. H. Long, and S. J. Bensmaia, "Neural Basis of Touch and Proprioception in Primate Cortex," in *Comprehensive Physiology*, 1st ed., Y. S. Prakash, Ed. Wiley, 2018, pp. 1575–1602.

[10] K. P. Blum *et al.*, "Diverse and complex muscle spindle afferent firing properties emerge from multiscale muscle mechanics," *eLife*, vol. 9, p. e55177, Dec. 2020.

[11] S. Kröger and B. Watkins, "Muscle spindle function in healthy and diseased muscle," *Skelet. Muscle*, vol. 11, no. 1, p. 3, Jan. 2021.

[12] K. N. Jaax and B. Hannaford, "A Biorobotic Structural Model of the Mammalian Muscle Spindle Primary Afferent Response," *Ann. Biomed. Eng.*, vol. 30, no. 1, pp. 84–96, Jan. 2002.

[13] R. Silva and T. Tabouillot, "Bio-electromechanical Model of the Muscle Spindle," in *2012 VI Andean Region International Conference*, Cuenca, Azuay, Ecuador, Nov. 2012, pp. 143–146.

[14] M. P. Mileusnic, I. E. Brown, N. Lan, and G. E. Loeb, "Mathematical Models of Proprioceptors. I. Control and Transduction in the Muscle Spindle," *J. Neurophysiol.*, vol. 96, no. 4, pp. 1772–1788, Oct. 2006.

[15] T. Rudjord, "A second order mechanical model of muscle spindle primary endings," *Kybernetik*, vol. 6, no. 6, pp. 205–213, Feb. 1970.

[16] S. W. Lee, D. Qiu, H. C. Fischer, M. O. Conrad, and D. G. Kamper, "Modulation of finger muscle activation patterns across postures is coordinated across all muscle groups," *J. Neurophysiol.*, vol. 124, no. 2, pp. 330–341, Aug. 2020.

[17] I. Williams and T. G. Constandinou, "Modelling muscle spindle dynamics for a proprioceptive prosthesis," *Annu. Int. Conf. IEEE Eng. Med. Biol. Soc.*, vol. 2013, pp. 1923–1926, Jul. 2013.

[18] H. Kajimoto, N. Kawakami, and S. Tachi, "Optimal design method for selective nerve stimulation and its application to electrocutaneous display," in *Proceedings 10th Symposium on Haptic Interfaces for Virtual Environment and Teleoperator Systems. HAPTICS 2002*, Orlando, FL, USA, 2002, pp. 303–310.

[19] G. B. Rollman, "Electrocutaneous stimulation: Psychometric functions and temporal integration," *Percept. Psychophys.*, vol. 5, no. 5, pp. 289–293, Sep. 1969.

[20] B. Geng, J. Dong, W. Jensen, S. Dosen, D. Farina, and E. N. Kamavuako, "Psychophysical evaluation of subdermal electrical stimulation in relation to prosthesis sensory feedback," *IEEE Trans. Neural Syst. Rehabil. Eng.*, vol. 26, no. 3, pp. 709–715, Mar. 2018.